Journal of Materials Chemistry C

Accepted Manuscript

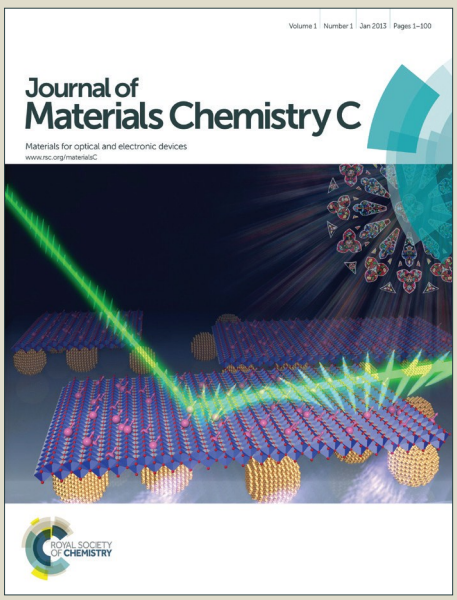

ROYAL SOCIETY OF CHEMISTRY

www.rsc.org/materialsC

Journal Name

ARTICLE TYPE

Cite this: DOI: 10.1039/xxxxxxxxxx

Temperature dependent structural, elastic, and polar properties of ferroelectric polyvinylidene fluoride (PVDF) and trifluoroethylene (TrFE) copolymers

Fu-Chang Sun,[a] Avinash M. Dongare,[b‡] Alexandru D. Asandei,[c‡] S. Pamir Alpay,[a,b‡] and Serge Nakhmanson*[a,b]

Received Date
Accepted Date

DOI: 10.1039/xxxxxxxxxx

www.rsc.org/journalname

We use molecular dynamics to calculate the structural, elastic, and polar properties of crystalline ferroelectric β-poly(vinylidene fluoride), PVDF (-CH_2-CF_2-)$_n$ with randomized trifluoroethylene TrFE (-CHF-CF_2-)$_n$ as a function of TrFE content (0-50%) in the temperature range of 0-400 K. There is a very good agreement between the experimentally obtained and the computed values of the lattice parameters, thermal expansion coefficients, elastic constants, polarization, and pyroelectric coefficients. A continuous decrease in Young's modulus with increasing TrFE content was observed and attributed to the increased intramolecular and intermolecular repulsive interactions between fluorine atoms. The computed polarization displayed a similar trend, with the room temperature spontaneous polarization decreasing by 44% from 13.8 μC/cm^2 (pure PVDF) to 7.7 μC/cm^2 [50/50 poly(VDF-*co*-TrFE)]. Our results show that molecular dynamics can be used as a practical tool to predict the mechanical and polarization-related behavior of ferroelectric poly(VDF-*co*-TrFE). Such an atomistic model can thus serve as a guide for practical applications of this important multifunctional polymer.

1 Introduction

Poly(vinylidene fluoride), PVDF (-CH_2-CF_2-)$_n$ and its copolymers with trifluoroethylene TrFE (-CHF-CF_2-)$_n$ or tetrafluoroethylene TFE (-CF_2-CF_2-)$_n$ stand out among the small number of known ferroelectric polymers due to their remarkable dielectric, piezoelectric and pyroelectric properties.[1–3] These outstanding electroactive characteristics have been exploited for a wide variety of applications, including biomedical,[4] energy storage,[5] sensors and actuators,[6] and filtration technologies.[7,8] Recent reports also emphasize excellent electrocaloric properties of PVDF and its TrFE copolymer, such as relatively high pyroelectric coefficients and low loss, making them attractive candidates for electrothermal energy harvesting where either the polymer by itself or a composite with a ceramic ferroelectric (*e.g.* $BaTiO_3$ or $Pb(Zr,Ti)O_3$) is used as a working medium.[9–12] Furthermore, relatively low ferroelectric-paraelectric transition temperature (343-413 K)[13] and the inherently large elastic, electrostrictive, and flexoelectric responses of poly(VDF-*co*-TrFE) provide additional degrees of freedom for the development of multifunctional electromechanical and electrothermal devices. Such advanced properties have also triggered efforts in the preparation of well-defined PVDF and its random and block copolymers using controlled radical polymerization methods.[14–17]

The initial interest in elucidating the mechanisms underpinning the remarkable electroactive properties of this polymer family was sparked by the pioneering work of Kawai[18] in 1969, who discovered strong piezoelectricity in the uniaxially-drawn and poled films, and that of Bergman *et al.*[19] in 1971, who reported pyroelectricity in PVDF. However, it was soon realized that on both microscopic and mesoscopic levels, the PVDF structure is quite complex, containing both crystalline and amorphous regions, and exhibiting a variety of phase transitions between different crystalline polymorphs under changing external conditions. Depending on chain conformation and molecular packing, PVDF may have at least four polymorphs: α (form II),[20] β (form I),[20] γ (form III)[21] and δ (form VI).[22] Both α and δ forms include TGTG′ (trans-gauche-trans-gauche) chain conformations, with α being non-polar and δ being polar due to different orderings of the monomer dipole moments. The ferroelectric β form con-

[a] *Department of Physics, University of Connecticut, Storrs, CT 06269-3046 USA. Fax:+1 860 486 3346; Tel:+1 860 486 4915; E-mail: smn@ims.uconn.edu*
[b] *Department of Materials Science and Engineering and Institute of Materials Science, University of Connecticut, Storrs, CT 06269-3136 USA Fax:+1 860 486 4745; Tel:+1 860 486 4620*
[c] *Department of Chemistry and Institute of Materials Science, University of Connecticut, Storrs, CT 06269-3060 USA. Fax:+1 860 486 2981; Tel:+1 860 486 2012*
‡ These authors contributed equally to this work.

sists of a quasihexagonal close-packed arrangement of polymer chains in all-trans (TTTT) conformation, with all the monomer units aligned along a single polar axis. Finally, the polar γ form, which can be considered an intermediate phase between α and β, is composed of T_3GT_3G' chain conformations.

PVDF polymorphs can be produced by a number of different processing techniques,[1] *e.g.*, the α phase can be readily synthesized by melt crystallization, while the β phase is normally obtained by the combination of mechanical stretching[23] and electrical poling[24] of α-crystalline PVDF. The γ phase is rather hard to access because it requires relatively high temperatures ($\sim$450K)[25] and long term annealing. The δ phase (first observed experimentally more than 40 years ago[24]) can be derived from the α phase by applying high electric fields (1.7MV/cm)[22] that induce the rotation of polymer chains about the backbone axis without any conformational changes. Utilization of higher electric fields ($\sim$5MV/cm) was reported to induce an α to β phase transition, accompanied by unfolding of all the gauche bonds into the TTTT chain conformation. Very recent results show that the δ phase can be stabilized via applying a short electrical pulse (2.5 MV/cm) to a thin film at the elevated substrate temperature (373 K).[26] The reported remnant polarization (7 μC/cm^2) and coercive field (1.15 MV/cm) are comparable to those of β-PVDF and poly(VDF-*co*-TrFE).

By virtue of its close-packed crystalline arrangement of the all-trans PVDF chains, among all the abovementioned PVDF polymorphs, the β phase should exhibit the highest polarization and commensurately high electroactive properties, such as piezo- and pyroelectricity. Indeed, this structure is regarded as a mainstay theoretical model for "simple" polymer ferroelectricity. However, experimentally grown β-PVDF samples usually require extensive post-processing to become ferroelectric and even after these procedures they still remain far from being perfectly ordered ($\sim$50-60%).[27] Nevertheless, it was shown that the β phase poly(VDF-*co*-TrFE) can be synthesized with a high degree of crystallinity ($\sim$90%) by increasing its TrFE content to 20-30%.[13,28,29]

During the two decades following the discovery of ferroelectricity in PVDF, a variety of classical interacting-dipole approaches had been used to evaluate the polarization and piezoelectric properties of this polymer family.[28,30–32] However, the output of these models was found to be inconsistent due to the lack of mechanisms accounting for redistribution of electronic charges, which could be accomplished only by quantum-mechanics based computational techniques. Nakhmanson *et al.*[33] have applied density functional theory (DFT) to study the polar properties of β-PVDF as a function of TrFE and TFE copolymer content, showing a large polarization enhancement within the crystal (as compared to the properties of individual all-trans PVDF chains) when quantum-mechanical effects are fully taken into account. Thereafter, DFT based methodology has been utilized, *e.g.*, by Wang *et al*,[34] who reported improved stability of the β phase in poly(VDF-*co*-TFE), and (with dispersion corrections) by Bohlén *et al.*[35], who show α and β as the most stable phases for pure PVDF and poly(VDF-*co*-TrFE), respectively. Furthermore, Pei *et al.*[36] have recently computed the structural and elastic properties for nine different polymorphs of PVDF.

Although a considerable amount of modeling effort was dedicated to elucidating the elastic, polar and piezoelectric properties of PVDF crystals, the dependence of these properties on both the copolymer content and temperature, *i.e.* parameters that are most important for potential electrothermal applications, has not been sufficiently addressed. Due to the complexity and partially disordered nature of the PVDF crystal structure, empirical force field (FF) potentials are currently the most efficient tools capable of providing quantitative predictions of the temperature-dependent physicochemical properties of PVDF and its copolymers at the molecular level. The first such field (called MSXX FF) was parameterized from quantum mechanical simulations for the four already existing, as well as for five theoretically predicted PVDF crystal forms by Karasawa and Goddard,[37] who also computed structural, elastic, and dielectric properties for the experimentally observed phases showing that they are in a good agreement with the information available at the time. Later, Carbeck *et al.* used a quasi-harmonic lattice dynamics approach combined with the Karasawa-Goddard MSXX FF potential to incorporate the effects of electronic polarization and dipole oscillations as a function of temperature.[38,39] A modified FF potential was developed by Tashiro *et al.*[40] to accurately reproduce the structural properties, vibrational frequencies, as well as the IR/Raman spectra of PVDF and poly(VDF-*co*-TrFE). The same group then studied the details of the ferroelectric to paraelectric phase transition[41,42] in poly(VDF-*co*-TrFE) as a function of copolymer content, demonstrating that polymers with larger VDF content have higher transition temperatures, which is consistent with experimental findings.

In this investigation, we conducted classical molecular dynamics (MD) simulations utilizing the well-established FF potential of Abe and Tashiro[42] to evaluate the elastic, polar and pyroelectric properties of β-PVDF as a function of temperature and TrFE comonomer amount. The aforementioned FF model has already been employed for simulations of the ferroelectric-to-paraelectric phase transitions in PVDF.[41–43] Here, we report the temperature-dependent lattice parameters, elastic stiffnesses and spontaneous polarization of the β-poly(VDF-*co*-TrFE) structure, as well as its thermal expansion and pyroelectric coefficients. The obtained structural and elastic properties are in good agreement with previous computational studies.[33,36,37,39] The computed spontaneous polarization exhibits a similar trend with increasing TrFE content as already predicted with the DFT calculations at 0K,[33] but its magnitude is underestimated by about 20%. However, the obtained pyroelectric coefficients of -2.5 to -3.76 (10^{-3} μC/cm^2 K^{-1}) are in good agreement with the reported experimental results, which range from -3.1 to -4.0 (10^{-3} μC/cm^2 K^{-1}).[44]

2 Methodology

2.1 Force Field

A FF potential is usually specified as a set of equations that describe all of the simulated interactions (including many body) between atoms within a crystal. The parameters of the FF employed in this investigation were taken from Abe, Tashiro, and Kobayashi,[45] which contains modifications from the orig-

inal paper of Tashiro *et al.*[40] providing more accurate estimates for the structural properties of PVDF and poly(VDF-*co*-TrFE). Utilizing the modified FF, Tashiro and coworkers have obtained the crystal structure and vibrational frequencies of α, β, and γ phases in agreement with the X-ray data, and studied the β phase ferroelectric-to-paraelectric phase transitional behavior.[42,43] They demonstrated that the modified potential can reproduce experimental phase transition temperatures, at least qualitatively accounting for the effects of chain packing and domain wall motion.

The total energy of the system within this FF can be expressed as

$$E = E_{val} + E_{nb} \tag{1}$$

where E_{val} represents all the bonded interactions (valence energy) and E_{nb} represents non-bonded interactions. These include

$$\begin{aligned} E_{val} &= E_b + E_a + E_t + E_{ab} + E_{bb} + E_{1aa} + E_{2aa} \\ E_{nb} &= E_{vdWij} + E_Q \end{aligned} \tag{2}$$

where valence energy E_{val} consists of E_b (bond stretch), E_a (angle bend), E_t (torsional), E_{ab} and E_{bb} (cross terms), E_{1aa} and E_{2aa} (angle-angle terms). Non-bonded energy E_{nb} consists of E_{vdWij} (van der Waals) and E_Q (Coulomb interactions). The 1-2 (bond) and 1-3 (angle) of Coulomb interactions are excluded because these interactions are covered in the valence energy terms. The detailed description of each energy expression can be found in the original work.[40] Proper incorporation of non-bonded interactions is essential for molecular dynamics simulations of polymer- and molecular crystal structures. On the other hand, the choice of an optimal cutoff range for such interactions involves achieving a balance between the simulations accuracy and computational time. We have tested the variations of the cutoff distance for non-bonding interactions within the FF and found negligible changes of the values of the property responses reported here.

2.2 Computational Details

The initial crystal structures for the PVDF and poly(VDF-*co*-TrFE) copolymer systems were generated using Moltemplate[46] and are shown in Fig. 1. The simulation box setup involved aligning the lattice parameters a, b, and c of the orthorhombic β-PVDF unit cell with Cartesian directions x, y, and z, respectively. In this setup, the y axis is parallel to the direction of the monomer dipole moments in β-PVDF, while the z axis is parallel to the direction of the polymer chain backbone. Different supercell geometries were tested to evaluate the influence of potential cell size effects on the properties under investigation. The simulation box size of $27\text{Å} \times 30\text{Å} \times 52\text{Å}$ ($\sim 3a \times 6b \times 20c$), *i.e.*, a arrangement of polymer chains each containing 20 monomers (720 monomers, 4320 atoms total), was found to be sufficiently large, *i.e.*, the change of the unit-cell lattice parameters upon further enlargement of the simulation box was below 0.1%.

Although, it is well known that abnormal linkages, e.g., inverted or head-to-head monomer arrangements, can occur in polymers during preparation,[47] in all the simulations presented here it is assumed that PVDF has a perfect head-to-tail monomer

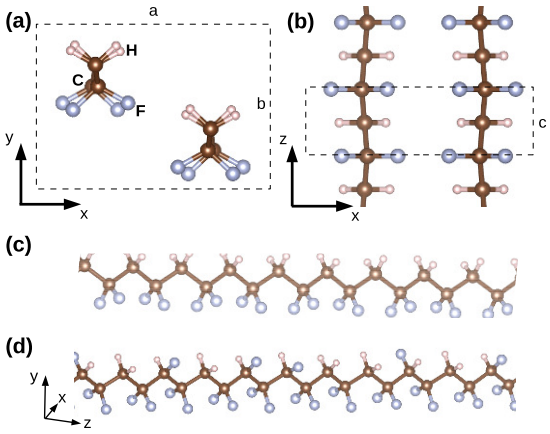

Fig. 1 The crystal structure of β-PVDF and its poly(VDF-*co*-TrFE) copolymer. β-PVDF chain packing shown in (a) x-y plane, and (b) x-z plane. The a, b, and c represent lattice constants. Polymer chain structures of (c) β-PVDF and (d) 50-50 randomized poly(VDF-*co*-TrFE) copolymer. Hydrogen (H) and carbon (C) atoms are represented by small ivory and medium-sized brown spheres, respectively. Fluorine (F) atoms are represented by large blue spheres.

arrangement, where the CH_2 unit (head) is always directly connected to the CF_2 unit (tail) along the polymer chain. An inverted VDF unit arrangement produces abnormal CH_2-CH_2 (head-to-head) and CF_2-CF_2 (tail-to-tail) linkages along the chain, with PVDF synthesized by free-radical polymerization typically containing one inverted unit per 10–20 regular units.[14–17,48]

Three-dimensional periodic boundary conditions (PBC) were applied in all simulations, while simulations involving cell shape and volume relaxation were conducted at a condition of vanishing shear stresses, *i.e.* of preserving the orthorhombic symmetry of the supercell. Fig. 1(a-b) shows the molecular structure and chain packing of the β-PVDF phase. To accommodate the effect of the steric hindrance between the adjacent fluorine pairs, in our initial models, alternating deflections away from the "planar backbone" symmetry were introduced in consecutive VDF units along each chain.[20] In Fig. 1(c-d), we illustrate the process of creating a random and atactic VDF-*co*-TrFE copolymer chain out of the pure PVDF, by substituting hydrogen atoms with fluorine. This procedure was used to prepare the initial configurations of poly(VDF-*co*-TrFE) copolymer-crystal structural models out of relaxed β-PVDF models.

All the energy terms discussed in the previous subsection were encoded in LAMMPS,[49] a classical MD simulation software package that was used to carry out all the calculations described herein. Standard Ewald summation was performed for non-bonded interactions within the cutoff distance of 7.6 Å. The PVDF crystal structure was optimized in a two-step process. On the first step, the system was relaxed to small ionic forces by the conjugate gradient (CG) algorithm in a fixed supercell until the energy change between successive iterations was less than 0.01%. In the second step, the final configuration from the previous step was relaxed further at a temperature below 0.01 K, using the NPT (isothermal-isobaric) ensemble with Parrinello-Rahman method[50] for pressure and temperature control, and

Nose-Hoover thermostats,[51,52] until the average of each stress tensor components was below 2 bar.

Nine independent components of the elastic stiffness tensor in the orthorhombic crystal system were evaluated at 0 K by introducing small (±0.5%) distortions to the shape of the simulation cell, and converging the resulting constrained structure back to small ionic forces and energy tolerances. Individual elastic stiffness components C_{ij} could then be computed from the obtained values of stresses σ_i and strains ε_j using the tensorial form of Hooke's law

$$\sigma_i = \sum_j C_{ij}\varepsilon_j \tag{3}$$

in conventional Voigt notation.[53]

To simulate the behavior of both the PVDF and poly(VDF-*co*-TrFE) at elevated temperatures, their structural models were equilibrated for 40,000 steps (20 picoseconds) after reaching the target temperature. At the end of that time interval, their properties were sampled for an NPT (isothermal-isobaric) ensemble.

The linear thermal expansion coefficients under constant applied stresses σ and electric field E were obtained as

$$\alpha_i = \frac{1}{x_i}\left(\frac{\partial x_i}{\partial T}\right)_{\sigma,E} \tag{4}$$

where x_i are the lattice parameters a, b, and c.[53]

Young's modulus along the chain direction E_c was computed by stretching the simulation box along the z-axis (by 2.5%) under fixed-volume condition. E_c is then obtained as the slope of stress-strain dependence

$$E_c = \sigma_c/\varepsilon_c \tag{5}$$

where σ_c and ε_c are the stress and strain along the chain direction, respectively.

The polarization of the polymer crystals was computed by the summation over the dipole moments of all the (VDF or TrFE) monomers within the supercell volume V

$$\mathbf{P} = \frac{1}{V}\sum_j \mu_\mathbf{j} = \frac{1}{V}\sum_i\sum_j q_i \mathbf{r_{ij}} \tag{6}$$

where μ_j is the dipole moment of monomer j, with q_i being the electric charge of atom i, and r_{ij} its Cartesian coordinate vector.

Pyroelectric coefficients along the polar (y) direction were then calculated under conditions of constant stresses and applied electric fields as

$$p_y^\sigma \equiv \left(\frac{\partial P_y}{\partial T}\right)_{\sigma,E} \tag{7}$$

where P_y is the polarization along the y-axis.

3 Analysis of Results

Prior to investigating the finite-temperature properties of the polymer crystals, we evaluated the self-energies of different PVDF phases at 0 K. Employing the β phase as a reference, the energies of the δ and α phases were found to be lower by 2.42 and 2.34 (kcal/mol per monomer unit), respectively. These values are consistent with the ones in Ref.[40]. Su *et al.*[54] have observed a similar trend with DFT calculations, reporting the energies of the δ and α phases that are lower than that of the β phase by 0.62 and 0.59 (kcal/mol per carbon atom), respectively. On the other hand, for the 50/50 poly(VDF-*co*-TrFE) copolymer, we found the energies of the δ and α phases to be higher than that of the β phase by 1.94 and 1.80 (kcal/mol per monomer unit), respectively. The same tendency was observed in DFT calculations,[54] with the energies of the δ and α phases being higher by 2.42 and 1.86 (kcal/mol per carbon unit). These results indicate that substituting hydrogen atoms with fluorines, and thus replacing VDF with TrFE, makes the β phase more energetically favorable, which is also observed experimentally.[13,29]

Table 1, presents the lattice parameters, density and spontaneous polarization for the β-PVDF and poly(VDF-*co*-TrFE) structural models considered in this investigation, at T = 0 K. Similar data from other computations is also included for comparison. Our results show that, with growing TrFE concentration, the along-the-backbone lattice parameter c remains rather constant, while the polar-direction lattice parameter b and the remaining lattice parameter a expand strongly, by up to 10% and 7%, respectively, in the 50/50 copolymer. The variation of the b and c lattice parameters is in general agreement with DFT-based calculations.[33] But the DFT predicted saturation of the lattice parameter a for TrFE concentrations above 20% is not observed in this investigation, which instead indicates its continuing expansion with increasing TrFE content. We should, however, point out that the poly(VDF-*co*-TrFE) structural models previously considered in the DFT investigation[33] were rather small (a 2 by 2 configuration of chains, each with 4 monomers), and not well randomized in the TrFE units position assignments at higher TrFE concentrations. Thus, they are most probably more tightly packed, by comparison with the better randomized large models utilized in this study.

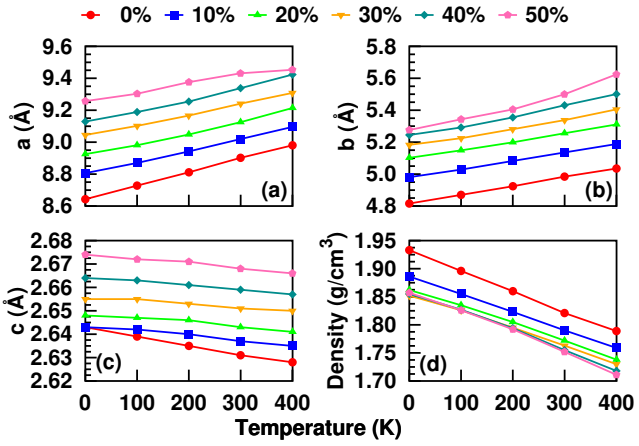

Fig. 2 β-PVDF and poly(VDF-*co*-TrFE) copolymer crystals lattice parameters a, b, and c, and density as functions of temperature.

The evolution of the β-PVDF and poly(VDF-*co*-TrFE) crystals density and lattice constants with changing temperature is presented in Fig. 2. As the temperature increases, lattice constants a and b expand, while lattice constant c contracts slightly (by ~0.01Å, due to small deviations of the polymer backbones away from the Z axis). This behavior can be attributed to highly anisotropic cohesive interactions within the crystals, *i.e.* the

Table 1 Lattice parameters, density, and polarization of PVDF and poly(VDF-*co*-TrFE)

TrFE(%)	Method	a(Å)	b(Å)	c(Å)	ρ(g/cm^2)	P_b(μC/cm^2)	Ref.
0	Exp	8.58	4.91	2.56	1.97	-	[55]
0	DFT	8.69	4.85	2.58	1.96	-	[36]
0	DFT	8.55	4.83	2.58	2.00	18.5	[33, 56]
0	FF	8.39	4.61	2.56	2.15	18.2	[39]
0	FF	8.79	4.88	2.63	1.89	-	[40]
0	FF (DFT)	8.64 (8.55)	4.82 (4.83)	2.64 (2.58)	1.93	14.9	This Work ([33])
10	FF (DFT)	8.81 (8.80)	4.98 (4.89)	2.64 (2.58)	1.89	13.1	This Work ([33])
20	FF (DFT)	8.93 (8.88)	5.10 (4.98)	2.65 (2.58)	1.86	11.7	This Work ([33])
30	FF (DFT)	9.05 (8.91)	5.18 (5.06)	2.66 (2.58)	1.85	10.5	This Work ([33])
40	FF (DFT)	9.13 (8.93)	5.25 (5.10)	2.66 (2.58)	1.86	9.3	This Work ([33])
50	FF (DFT)	9.26 (8.99)	5.28 (5.18)	2.67 (2.58)	1.86	8.3	This Work ([33])

strong covalent bonding between monomers along the polymer chain vs. weak non-bonding between individual chains. The density of each polymer crystal gradually decreases with increasing temperature. At room temperature, we obtain values in the range of 1.75-1.85 g/cm^3 that are consistent with reported experimental results of 1.68 to 1.97 g/cm^3, depending on the crystallinity of the sample.[48]

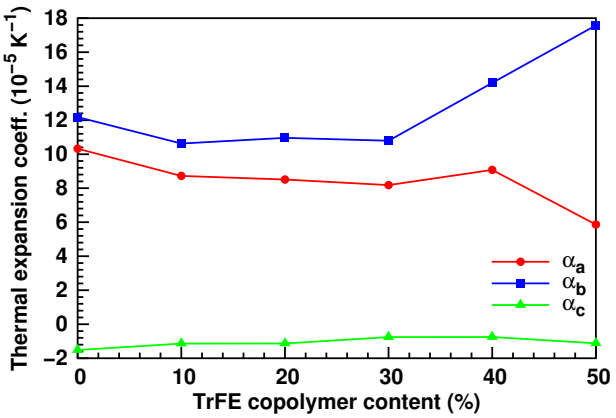

Fig. 3 Room-temperature thermal expansion coefficients of β-PVDF and poly(VDF-*co*-TrFE) copolymer crystals as functions of the TrFE content.

The dependence of the room temperature thermal expansion coefficients on the TrFE copolymer content, obtained from the variation of the lattice constants presented in Fig. 2, is shown in Fig. 3. The values of the expansion coefficients α_a and α_b are much larger than that of α_c. Moreover, α_c, which is along the chain direction, is negative and an order magnitude smaller than the others. Carbeck and Rutledge[39] reported similar values of the thermal expansion coefficients, including slight contraction along the chain direction with increasing temperature.

Although PVDF-based polymers have been studied for decades, their elastic properties remain elusive. This is due not only to partial crystallinity of PVDF or its structural complexity, but also to a wide variety of morphologically different samples that have been produced over the years utilizing a broad range of synthetic techniques.[48]

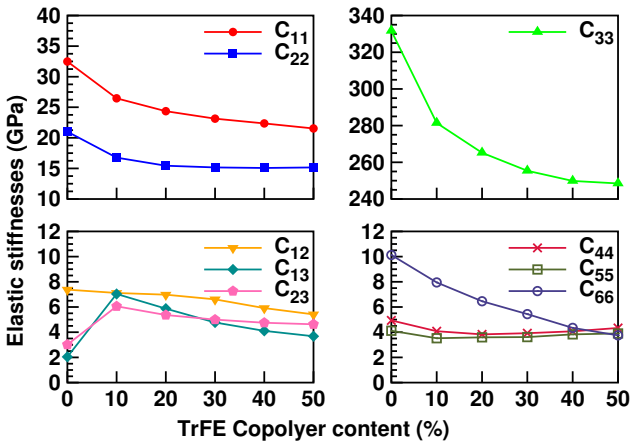

Fig. 4 Elastic stiffness tensor components of the β-PVDF and poly(VDF-*co*-TrFE) crystals as functions of TrFE copolymer content.

The components of the elastic stiffness tensor for the β-PVDF crystal are presented in Table 2. The results of other known calculations are also provided for comparison and are in general agreement with our findings.[57] The dependence of the values of the elastic stiffness tensor components of poly(VDF-*co*-TrFE) on composition are shown in Fig. 4. As expected, for all TrFE concentrations, the elastic stiffness component along backbone chain direction C_{33} remains about an order of magnitude larger, compared to the other two principal direction components C_{11} and C_{22}. The rest of the elastic stiffness components are an order of magnitude smaller, compared to the latter two components. Increasing the TrFE percentage results in a substantial drop in the copolymer stiffness, with the C_{11}, C_{22} and C_{33} components declining by up to 50, 30 and 25%, respectively, for the 50/50 system. This can be attributed to the disordering of the polymer crystal structure under the influence of increasing repulsive forces between and/or within the chains.[13] The experimental value of C_{33} in β-PVDF film was reported to be 177 GPa using X-ray diffraction under the assumption of homogeneous stress.[59] This is substantially lower than values of 280–330 GPa reported in this, and other computational studies.[36,37,39,57,58] This discrepancy can be explained by the fact that the type of randomness present even in large computational models of β-PVDF crystals includes only ro-

Table 2 Elastic stiffness tensor (GPa) of pure PVDF

Method	C_{11}	C_{22}	C_{33}	C_{44}	C_{55}	C_{66}	C_{12}	C_{13}	C_{23}	Ref.
EXP(10 K)	11.9	15.6	121	4.5	4.5	3.0	-	-	-	[57]
DFT	19.8	24.5	287	1.2	0.3	1.7	4.3	0.8	3.3	[36]
FF	23.2	10.6	237	2.2	4.4	6.4	-	-	-	[58]
FF	25.5	12.4	283	3.5	5.1	4.0	3.0	4.0	2.4	[37]
FF	31.0	32.9	293	-	-	-	2.9	4.7	8.5	[39]
FF	32.5	21.0	332	4.9	4.1	10.0	7.4	2.0	3.0	This Work

tational disordering of the polymer chains, which still remain perfectly aligned and connected along the backbone direction. Furthermore, with the exception of the head-to-head (HH) monomer arrangements, most other types of defects and impurities present in experimentally grown samples[58] are also usually not considered in such models. Moreover, the elastic properties measured in various PVDF samples that are prepared by different experimental approaches, would also lead to differing results.[60] Finally, the computational results reported here were obtained using a FF with fixed ionic charges, which in reality are likely to vary with changing temperature, as well as with distortions of bonds and angles between ions. More accurate simulation techniques, e.g., *ab initio* MD, can correctly account for ionic charge variations, however, these simulations are currently extremely demanding for the large time and length scales involved in the modeling of polymer-crystal structures, such as the ones considered in this investigation.

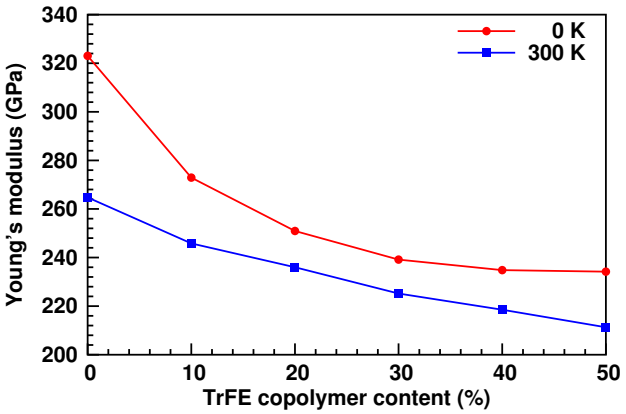

Fig. 5 Young's modulus E_c along the polymer chain direction as a function of the TrFE copolymer content at 0 K and room temperature.

Fig. 5 shows the dependence of Young's modulus E_c in poly(VDF-*co*-TrFE) system at 0 K and room temperature on the TrFE concentration. Due to thermal expansion, E_c is lower at elevated temperatures. Furthermore, the presence of TrFE monomers significantly decreases the Young's modulus value. This effect is most pronounced at smaller copolymer compositions, which could be attributed to the initial rotational disordering of the polymer chains.

In terms of polar properties, Fig. 6 presents the results of our (point-charge based model)[58] calculations of spontaneous polarization at 0 K and room temperature as the function of TrFE concentration. Comparisons to the results of the DFT calculations[33] (at 0 K), as well as some experimental measurements for a variety of different samples are also included. Here, the FF combined with point-charge based dipole-moment computations reproduce the rate of decrease of the spontaneous polarization with increasing TrFE content, but these values are systematically underestimated vs. DFT values by as much as ∼20% for the whole range of TrFE compositions. It is also noteworthy that the results of most experimental measurements assembled in Fig. 6, which are presumably made for not fully crystalline and defect-free samples, also appear higher than the polarization values produced by this FF. At the same time, our results suggest that within the approximations of the utilized computational approach, the change in temperature from 0 to 300 K introduces only a marginal, ∼7% decrease in polarization, which is mostly due to the thermal expansion of the simulation box. Therefore, the presented results demonstrate that in order to correctly simulate the polarization in such systems a successful FF parameterization (*e.g.*, such as the one introduced for PVDF in Ref.[33]) has to account for the contributions of the electronic degrees of freedom, *i.e.*, the polarization of electron clouds on the monomer under the influence of the internal electric field produced by the dipole moments of monomers around it. However, it may still be possible to obtain reasonable estimates for certain polarization-related properties

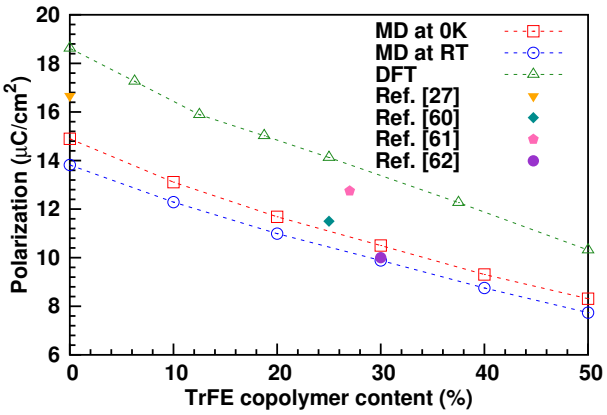

Fig. 6 Polarization of the β-PVDF and poly(VDF-*co*-TrFE) crystals as a function of TrFE copolymer content at 0 K and room temperature(RT). Data from the DFT-based calculations of Ref.[33] (at 0 K) and experimental results of β-PVDF file from Ref.[27], 75-25% poly(VDF-*co*-TrFE) polycrystalline film from Ref.[61], 73-27% sample from Ref.[62], and 70-30% poly(VDF-*co*-TrFE) film from Ref.[63], are also shown for comparison.

that depend on polarization derivatives rather than on absolute values.

Table 3 Pyroelectric coefficient (10^{-3} μC/cm^2 K^{-1}) at room temperature

TrFE(%)	0	10	20	30	40	50
p_y^σ	-3.76	-2.89	-2.53	-2.97	-2.30	-2.50

As suggested by our further computations, the pyroelectric coefficient of β-PVDF is one of such properties. Table 3 presents the obtained values for the dependence of the room temperature pyroelectric coefficient on copolymer composition. Our result for β-PVDF compares favorably to the reported value -3.26 (10^{-3} μC/cm^2 K^{-1}) in another theoretical study[39] and -2.6∼-3.5 (10^{-3} μC/cm^2 K^{-1}) from the experimental measurements.[64,65] While we predict smaller pyroelectric coefficients in poly(VDF-*co*-TrFE) copolymer crystals, this declining trend is not monotonous, displaying a relatively large pyroelectric response in the 70/30 system.

4 Conclusions

Finite temperature MD simulations of the structural, elastic, polar and pyroelectric properties of ferroelectric β-PVDF and of poly(VDF-*co*-TrFE) of various compositions were carried out. A refined FF of Tashiro *et al.*[40,45] was utilized in all the calculations. Our study demonstrates that this FF reproduces the structural, pyroelectric and, in the absence of experimental data, some of the elastic characteristics of highly crystalline β-PVDF and copolymers. However, the spontaneous polarization, obtained through point-charge summation over the ionic coordinates produced by the FF, is underestimated by ∼20% for all the copolymer compositions. Therefore, a further modification of this FF, *e.g.*, by augmenting it using a shell model, will be very useful for further modeling of polar, piezoelectric and electrocaloric properties of these materials. Moreover, the inclusion of HH PVDF defects, as well as that of polymer chain ends will lead to further refinement of our models. Research along these lines is in progress and will be reported in due time.

References

1 K. Tashiro, *Ferroelectric Polymers: Chemistry: Physics, and Applications*, Marcel Dekker, New York, 1995, pp. 63–181.
2 A. J. Lovinger, *Science*, 1983, **220**, 1115–1121.
3 J. F. Legrand, *Ferroelectrics*, 1989, **91**, 303–317.
4 R. Costa, C. Ribeiro, A. C. Lopes, P. Martins, V. Sencadas, R. Soares and S. Lanceros-Mendez, *Journal of Materials Science: Materials in Medicine*, 2013, **24**, 395–403.
5 J. Nunes-Pereira, A. C. Lopes, C. M. Costa, L. C. Rodrigues, M. M. Silva and S. Lanceros-Méndez, *Journal of Electroanalytical Chemistry*, 2013, **689**, 223–232.
6 Y. Bar-Cohen and Q. Zhang, *MRS Bulletin*, 2008, **33**, 173–181.
7 P. Martins, X. Moya, L. C. Phillips, S. Kar-Narayan, N. D. Mathur and S. Lanceros-Mendez, *Journal of Physics D: Applied Physics*, 2011, **44**, 482001–482004.
8 P. Martins, A. C. Lopes and S. Lanceros-Mendez, *Progress in Polymer Science*, 2014, **39**, 683–706.
9 C. S. Lee, J. Joo, S. Han and S. K. Koh, *Applied Physics Letters*, 2004, **85**, 1841–1843.
10 K. Ken-ichi, F. Keisuke and O. Hidetoshi, *Sensors & Actuators: A. Physical*, 2013, **200**, 21–25.
11 S. P. Alpay, J. Mantese, S. Trolier-McKinstry, Q. Zhang and R. W. Whatmore, *MRS Bulletin*, 2014, **39**, 1099–1111.
12 D. Jun Li, S. Hong, S. Gu, Y. Choi, S. Nakhmanson, O. Heinonen, D. Karpeev and K. No, *Applied Physics Letters*, 2014, **104**, 012902–012905.
13 T. Furukawa, *Phase Transitions*, 1989, **18**, 143–211.
14 A. D. Asandei, C. P. Simpson, O. I. Adebolu and Y. Chen, in *Towards Metal Mediated Radical Polymerization of Vinylidene Fluoride*, American Chemical Society, 2012, ch. 5, pp. 47–63.
15 A. D. Asandei, O. I. Adebolu and C. P. Simpson, *Journal of the American Chemical Society*, 2012, **134**, 6080–6083.
16 A. D. Asandei, O. I. Adebolu, C. P. Simpson and J. S. Kim, *Angewandte Chemie - International Edition*, 2013, **52**, 10027–10030.
17 A. D. Asandei, O. I. Adebolu and C. P. Simpson, In D. W. Smith et al. (Ed.) *Handbook of fluoropolymer science and technology*, John Wiley & Sons, Inc., 2014, pp. 21–42.
18 H. Kawai, *Japanese Journal of Applied Physics*, 1969, **8**, 975–976.
19 J. G. Bergman, J. H. McFee and G. R. Crane, *Applied Physics Letters*, 1971, **18**, 203–205.
20 R. Hasegawa, Y. Takahashi, Y. Chatani and H. Tadokoro, *Polymer Journal*, 1972, **3**, 600–610.
21 A. J. Lovinger, *Macromolecules*, 1981, 322–325.
22 M. Bachmann, W. L. Gordon, S. Weinhold and J. B. Lando, *Journal of Applied Physics*, 1980, **51**, 5095–5099.
23 V. Sencadas, R. Gregorio and S. Lanceros-Mendez, *Journal of Macromolecular Science Part B*, 2009, **48**, 514–525.
24 G. T. Davis, J. E. McKinney, M. G. Broadhurst and S. C. Roth, *Journal of Applied Physics*, 1978, **49**, 4998–5002.
25 S. Weinhold, M. H. Litt and B. Lando, *American Chemical Society*, 1980, **13**, 1178–1183.
26 M. Li, H. J. Wondergem, M.-J. Spijkman, K. Asadi, I. Katsouras, P. W. M. Blom and D. M. de Leeuw, *Nature materials*, 2013, **12**, 433–438.
27 K. Nakamura, D. Sawai, Y. Watanabe, D. Taguchi, Y. Takahashi, T. Furukawa and T. Kanamoto, *Journal of Polymer Science Part B: Polymer Physics*, 2003, **41**, 1701–1712.
28 T. Yagi, M. Tatemoto and J.-i. Sako, *Polymer Journal*, 1980, **12**, 209–223.
29 K. Koga and H. Ohigashi, *Journal of Applied Physics*, 1986, **59**, 2142–2150.
30 H. Kakutani, *Journal of Polymer Science Part A-2: Polymer Physics*, 1970, **8**, 1177–1186.
31 R. Al-Jishi and P. L. Taylor, *Journal of Applied Physics*, 1985, **57**, 902–905.
32 C. K. Purvis and P. L. Taylor, *Journal of Applied Physics*, 1983, **54**, 1021–1028.

33 S. M. Nakhmanson, M. B. Nardelli and J. Bernholc, *Physical Review B*, 2005, **72**, 115210–115217.

34 Z.-Y. Wang, K.-H. Su, H.-Q. Fan and Z.-Y. Wen, *Polymer*, 2007, **48**, 7145–7155.

35 M. Bohlén and K. Bolton, *Physical Chemistry Chemical Physics*, 2014, **16**, 12929–12939.

36 Y. Pei and X. C. Zeng, *Journal of Applied Physics*, 2011, **109**, 093514–093520.

37 N. Karasawa and W. A. I. I. I. Goddard, *Macromolecules*, 1992, **25**, 7268–7281.

38 J. D. Carbeck, D. J. Lacks and G. C. Rutledge, *The Journal of Chemical Physics*, 1995, **103**, 10347–10355.

39 J. D. Carbeck and G. C. Rutledge, *Polymer*, 1996, **37**, 5089–5097.

40 K. Tashiro, Y. Abe and M. Kobayashi, *Ferroelectrics*, 1995, **171**, 281–297.

41 Y. Abe and K. Tashiro, *Polymer*, 2001, **42**, 3409–3417.

42 Y. Abe and K. Tashiro, *Polymer*, 2001, **42**, 9671–9678.

43 Y. Abe and K. Tashiro, *Journal of Polymer Science Part B: Polymer Physics*, 2001, **39**, 689–702.

44 N. Neumann, R. Köhler and G. Hofmann, *Integrated Ferroelectrics*, 1995, **6**, 213–230.

45 Y. Abe, K. Tashiro and M. Kobayashi, *Computational and Theoretical Polymer Science*, 2000, **10**, 323–333.

46 A. Jewett and J. Lambert, *Moltemplate (Version 1.29) [Computer software]*, 2015.

47 O. Vogl, M. F. Qin and a. Zilkha, *Progress in Polymer Science (Oxford)*, 1999, **24**, 1481–1525.

48 B. Ameduri, *Chemical Reviews*, 2009, **109**, 6632–6686.

49 S. Plimpton, *Journal of Computational Physics*, 1995, **117**, 1–19.

50 M. Parrinello and A. Rahman, *Journal of Applied Physics*, 1981, **52**, 7182–7190.

51 W. G. Hoover, *Physical Review A*, 1985, **31**, 1695–1697.

52 S. Nosé, *The Journal of Chemical Physics*, 1984, **81**, 511–519.

53 J. F. Nye, *Physical Properties of Crystals: Their Representation by Tensors and Matrices*, Clarendon Press, 1985.

54 H. B. Su, A. Strachan and W. A. Goddard, *Physical Review B*, 2004, **70**, 064101–064108.

55 J. B. Lando, H. G. Olf and A. Peterlin, *Journal of Polymer Science Part A-1: Polymer Chemistry*, 1966, **4**, 941–951.

56 S. M. Nakhmanson, R. Korlacki, J. T. Johnston, S. Ducharme, Z. Ge and J. M. Takacs, *Physical Review B*, 2010, **81**, 174120–174127.

57 K. Omote, H. Ohigashi and K. Koga, *Journal of Applied Physics*, 1997, **81**, 2760–2769.

58 K. Tashiro, M. Kobayashi, H. Tadokoro and E. Fukada, *Macromolecules*, 1980, **13**, 691–698.

59 I. Sakurada and K. Kaji, *Journal of Polymer Science Part C: Polymer Symposia*, 1970, **31**, 57–76.

60 R. F. Schaufele and T. Shimanouchi, *The Journal of Chemical Physics*, 1967, **47**, 3605–3610.

61 H. Ohigashi, K. Omote and T. Gomyo, *Applied Physics Letters*, 1995, **66**, 3281–3283.

62 Y. Tajitsu, H. Ogura, A. Chiba and T. Furukawa, *Japanese Journal of Applied Physics*, 1987, **26**, 554–560.

63 H. Kliem and R. Tadros-Morgane, *Journal of Physics D: Applied Physics*, 2005, **38**, 1860–1868.

64 A. V. Bune, C. Zhu, S. Ducharme, L. M. Blinov, V. M. Fridkin, S. P. Palto, N. G. Petukhova and S. G. Yudin, *Journal of Applied Physics*, 1999, **85**, 7869–7873.

65 H. H. S. Chang and Z. Huang, *Journal of Applied Physics*, 2009, **106**, 014101–014109.